

Physical-layer secrecy outage of spectrum sharing CR systems over fading channels

Hequn LIU¹, Hui ZHAO¹, Hong JIANG¹, Chaoqing TANG¹,
Gaofeng PAN^{1*}, Tingting LI² & Yunfei CHEN³

¹Chongqing Key Laboratory of Nonlinear Circuits and Intelligent Information Processing,
Southwest University, Chongqing 400715, China;

²School of Mathematics and Statistics, Southwest University, Chongqing 400715, China;

³School of Engineering, University of Warwick, Coventry CV4 7AL, U.K.

Received July 12, 2015; accepted August 30, 2015; published online March 16, 2016

Abstract In this paper, we investigate the physical-layer secrecy outage performance of underlay spectrum sharing systems over Rayleigh and log-normal fading channels in the presence of one eavesdropper. In particular, the secondary transmitter sends data to the legitimate receiver under the constraints of the interference temperature at the primary receiver, while suffering the wiretap from the eavesdropper. Closed-form and approximated expressions are derived for the secrecy outage probability over Rayleigh and log-normal fading channels, respectively. The accuracy of our performance analysis is verified by simulation results.

Keywords spectrum sharing, cognitive radio, secrecy outage probability, Rayleigh fading channels, log-normal fading channels

Citation Liu H Q, Zhao H, Jiang H, et al. Physical-layer secrecy outage of spectrum sharing CR systems over fading channels. *Sci China Inf Sci*, 2016, 59(10): 102308, doi: 10.1007/s11432-015-5451-2

1 Introduction

Nowadays, physical-layer (PHY) security has emerged as a key technique to provide trustworthiness and reliability for future wireless transmissions due to the broadcast nature of wireless transmission. Differing from traditional cryptographic approaches, the main idea of PHY security is to exploit the wireless channel's PHY characteristics, such as fading, noise or interference, to realize secure communications. More specifically, it is to increase the channel capacity difference between the main and eavesdropping links, as shown by Wyner's wiretap model [1].

The study on Wyner's wiretap model has been extended for various network scenarios, e.g., signal-input signal-output (SISO) [2] and multi-input multi-output over independent Rayleigh fading channels [3–5], SISO over correlated Rayleigh [6] and log-normal fading channels [7–9].

Recently, cognitive radio (CR) has been proposed and regarded as a promising technique to solve the spectrum shortage problem or to improve the spectrum efficiency in future wireless communication systems [10]. Secondary users are allowed to access to the licensed spectrum of the primary user in

* Corresponding author (email: gfp@swu.edu.cn)

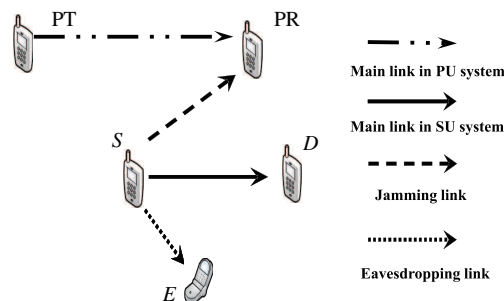


Figure 1 System model.

spectrum sharing systems, while the interference power generated by the secondary user does not interfere with the primary user's communications.

Some other researchers noticed the PHY security in CR system and have proposed some findings on this issue [11–14]. In [11], the authors gave an overview on several existing security attacks to the PHY in CR networks and investigated the secrecy capacity and the secrecy outage probability of a primary user. The authors of [12] investigated the PHY security against eavesdropping attacks in CR networks with multiple eavesdroppers and proposed a user scheduling scheme to achieve multiuser diversity for improving the security level of cognitive transmissions with a primary quality of service constraint. A relay selection scheme was proposed for the security constrained CR networks with single eavesdropper, multiple eavesdroppers and primary users in [13]. The authors of [14] presented the PHY approaches to defense against security threats in CR networks, which can be valid not only for the attacks in the PHY but also for those in the upper layer.

However, none of the work has studied the PHY secrecy outage performance of spectrum sharing systems. In [15], the secrecy outage performance of underlay CR systems has been studied over Nakagamin- m fading channels. It is clear that the analytical results were derived using the interference temperature limit without considering the maximum transmitting power constraint at the secondary user. By considering secondary receiver and the eavesdropper equipped with multiple antennas, closed-form expressions for the exact and asymptotic secrecy outage probability were derived for underlay CR systems. However, the method adopted in [16] is quite complicated in deriving the probability density function (PDF) of the instantaneous Signal-to-Noise-Ratio (SNR) at primary user's receiver and secondary user's receiver as shown by Eq. (12) in [16], which reduced the readability of that work.

Motivated by above observations, in this work, we consider the Wyner's wiretap model under the spectrum sharing scenarios, as shown in Figure 1. Then, the transmitting power at the secondary user is limited not only due to the interference power requirement (namely, the interference temperature) at the primary receiver but also due to its maximum available transmitting power. Other than the method that derives the PDF of the instantaneous SNR at primary user's receiver and secondary user's receiver [16], the secrecy outage performance is studied in the presence of an eavesdropper under two cases, which is based on the power constraint at the secondary user's receiver, and the approximated closed-form expressions of secrecy outage probability (SOP) have been derived for Rayleigh and log-normal fading scenarios, respectively.

The rest of this paper is organized as follows. In Section 2, we introduce the considered underlay spectrum sharing system model. In Section 3, we study SOP and derive the closed-form and approximated expressions for SOP. In Section 4, we present numerical and simulation results to validate the accuracy of our proposed analytical models. Section 5 finally concludes the paper.

2 System and signal models

In this paper, we consider an underlay spectrum sharing system with one primary transmitter (PT) sending confidential messages to one primary receiver (PR), as shown in Figure 1. The secondary system consists of one source (S), one destination (D) and an eavesdropper (E) located around S attempting

to capture the confidential messages transmitted by S . We assume that D and E are far from PT, thus, the received signals at D and E will not be interfered by the primary users. Under underlay spectrum sharing mode, S and D can access to the licensed spectrum of the primary user, only when the interference generated by the secondary user does not exceed the pre-defined threshold at PR.

The received signal at D and E can be given by

$$y_{S,D} = \sqrt{P_S} h_{S,D} \cdot X_S + n_D, \tag{1}$$

$$y_{S,E} = \sqrt{P_S} h_{S,E} \cdot X_S + n_E, \tag{2}$$

respectively, where P_S is the transmitting power at S ; $h_{i,j}$ denotes the channel coefficient for the link from nodes i and j ($i, j \in \{S, D, PR, E\}$); X_S is the transmitted symbol at S , i.e., $X_S \in \{+1, -1\}$ while binary phase shift keying modulation is adopted; n_D and n_E are the complex additive white Gaussian noise (AWGN) with zero mean and variance σ^2 at D and E , respectively.

3 Secrecy outage probability

In order not to degrade the QoS of PR, the transmitting power at S (P_S) should be limited at a given threshold (I_P) that the PR can tolerate, thus P_S can be written as

$$P_S = \begin{cases} I_P/g_P, & P_M \geq I_P/g_P \Rightarrow g_P \geq I_P/P_M; \\ P_M, & P_M < I_P/g_P \Rightarrow g_P < I_P/P_M, \end{cases} \tag{3}$$

where $g_P = |h_{S,PR}|^2$ is the channel power gain between S and PR, and P_M is the maximal transmitting power at S .

Let $\gamma_{S,i}$ represent the SNR of the link S -to- i ($i \in \{PR, D, E\}$). Then, we have

$$\gamma_{S,i} = P_S |h_{S,i}|^2 / \sigma^2. \tag{4}$$

Thus, the instantaneous secrecy capacity for link S - D can be expressed as

$$C_S = \log_2(1 + \gamma_{SD}) - \log_2(1 + \gamma_{SE}). \tag{5}$$

In this paper we define SOP as the probability that the instantaneous secrecy capacity C is below a target secrecy rate C_{th} . Differing from [16], we can calculate SOP under the two cases of P_S as suggested by (3) as

$$\begin{aligned} \text{SOP}(C_{th}) &= \Pr\{g_P \geq I_P/P_M\} \text{SOP}_1(C_{th}) \\ &\quad + \Pr\{g_P < I_P/P_M\} \text{SOP}_2(C_{th}), \end{aligned} \tag{6}$$

where $\text{SOP}_1(C_{th})$ and $\text{SOP}_2(C_{th})$ refer to the SOP when $P_S = I_P/g_P$ and $P_S = P_M$, respectively.

Let h_1, h_2 and h_3 denote $h_{S,PR}, h_{S,D}$ and $h_{S,E}$ for simplification. When $g_P \geq I_P/P_M$, SOP_1 can be given by

$$\begin{aligned} \Pr\{C_S \leq C_{th}\} &= \Pr\left\{\frac{(\alpha - 1)g_P + \alpha\rho g_E}{\rho g_D} \geq 1\right\} \\ &= \Pr\{(\alpha - 1)g_P + \alpha\rho g_E \geq \rho g_D\} \\ &= \Pr\left\{\frac{\alpha - 1}{\rho}g_P \geq g_D - \alpha g_E\right\}, \end{aligned} \tag{7}$$

where $g_D = |h_2|^2$, $g_E = |h_3|^2$, $\rho = I_P/\sigma^2$ and $\alpha = 2^{C_{th}}$.

3.1 Rayleigh fading channels

It is assumed that all links experience independent and identically distributed (i.i.d.) Rayleigh fading, $h_i \sim \mathcal{CN}(0, \sigma_i)$ ($i \in \{1, 2, 3\}$), where σ_i^2 is the variance.

As h_i follows Rayleigh distribution, we have $|h_i|^2$ follow exponential distribution, $|h_i|^2 \sim \exp(\lambda_i)$, where $i \in \{P, D, E\}$ and $\lambda_i = \frac{1}{2\sigma_i^2}$.

3.1.1 The derivation of SOP_1

Let $Z_1 = \frac{\alpha-1}{\rho}g_P$, $Z_2 = g_D - \alpha g_E$, $X = \alpha g_E$. The PDF of g_P , X and Z_1 can be given by

$$f(g_P | g_P \geq I_P/P_M) = \frac{f(g_P)}{1 - F(I_P/P_S)} = A \cdot \lambda_P \exp(-\lambda_P g_P) = A \cdot f(g_P), g_P \geq I_P/P_M, \quad (8)$$

$$f_X(x) = \frac{\exp(-\lambda_E x/\alpha) \lambda_E}{\alpha}, \quad (9)$$

$$f_{Z_1}(z_1) = \frac{A\rho}{\alpha-1} f_{g_P}\left(\frac{\rho z_1}{\alpha-1}\right) = \frac{A\rho\lambda_P}{\alpha-1} \exp\left(-\frac{\lambda_P \rho z_1}{\alpha-1}\right), z_1 \geq \frac{(\alpha-1)\sigma^2}{P_M} = B, \quad (10)$$

where $A = 1/\exp(-\lambda_P I_P/P_M)$, respectively.

Using Eq. (6-55) in [17], when $Z_2 \geq 0$, we can derive the PDF of Z_2 as

$$f_{Z_2}(z_2) = \int_0^\infty f_{g_D X}(z_2 + x, x) dx = \int_0^\infty f_{g_D}(z_2 + x) f_X(x) dx. \quad (11)$$

Substituting the PDFs of g_D and X into (11), we can get

$$f_{Z_2}(z_2) = \frac{\lambda_D \lambda_E \exp(-\lambda_D z_2)}{\alpha} \int_0^\infty \exp\left[-\left(\lambda_D + \frac{\lambda_E}{\alpha}\right)x\right] dx = \frac{\Omega \exp(-\lambda_D z_2)}{\lambda_D + \lambda_E/\alpha}, \quad (12)$$

where $\Omega = \frac{\lambda_D \lambda_E}{\alpha}$.

Then we can rewrite (7) as

$$\begin{aligned} SOP(C_{th}) &= \int_B^\infty f_{Z_1}(z_1) \int_{-\infty}^{z_1} f_{Z_2}(z_2) dz_2 dz_1 \\ &= \underbrace{\int_B^\infty f_{Z_1}(z_1) \int_{-\infty}^0 f_{Z_2}(z_2) dz_2 dz_1}_{I_1} + \underbrace{\int_B^\infty f_{Z_1}(z_1) \int_0^{z_1} f_{Z_2}(z_2) dz_2 dz_1}_{I_2}. \end{aligned} \quad (13)$$

Considering the following integral equation:

$$\int_0^\infty f_{Z_2}(z_2) dz_2 = \int_0^\infty \frac{\Omega \exp(-\lambda_D z_2)}{\lambda_D + \lambda_E/\alpha} dz_2 = \frac{\Omega}{\lambda_D^2 + \Omega}, \quad (14)$$

it is easy to observe that $I_1 = 1 - \frac{\Omega}{\lambda_D^2 + \Omega}$.

I_2 can be written as

$$I_2 = \frac{\Omega}{(\lambda_D + \lambda_E/\alpha)} \int_B^\infty f_{Z_1}(z_1) \int_0^{z_1} \exp(-\lambda_D z_2) dz_2 dz_1. \quad (15)$$

Substituting the PDF of Z_1 into (15), we can get

$$I_2 = \frac{\Omega}{\lambda_D (\lambda_D + \lambda_E/\alpha)} \frac{A\rho\lambda_P}{\alpha-1} \left\{ \frac{\alpha-1}{\lambda_P \rho} \exp\left(-\frac{\lambda_P \rho B}{\alpha-1}\right) - \frac{\exp\left[-\left(\lambda_D + \frac{\rho}{\alpha-1}\right)B\right]}{\left(\lambda_D + \frac{\rho}{\alpha-1}\right)} \right\}. \quad (16)$$

Finally, SOP_1 can be given by

$$\begin{aligned} SOP_1(C_{th}) &= 1 - \frac{\Omega}{\left(\lambda_D^2 + \frac{\lambda_E \lambda_P}{\alpha}\right)} + \frac{\Omega}{\lambda_D (\lambda_D + \lambda_E/\alpha)} \frac{A\rho\lambda_P}{\alpha-1} \left\{ \frac{\alpha-1}{\lambda_P \rho} \exp\left(-\frac{\lambda_P \rho B}{\alpha-1}\right) \right. \\ &\quad \left. - \frac{\exp\left[-\left(\lambda_D + \frac{\rho}{\alpha-1}\right)B\right]}{\left(\lambda_D + \frac{\rho}{\alpha-1}\right)} \right\}. \end{aligned} \quad (17)$$

3.1.2 The derivation of $SOP_2(C_{th})$

When $g_P < I_P/P_M$, $P_S = P_M$. It means that S only adopts its maximal transmitting power to deliver information to D . Obviously, the target system model falls into non-CR model in this case.

Substituting $\gamma_M = P_M g_D/\sigma^2$, $\bar{\gamma}_M = P_M/(\sigma^2 \lambda_2)$, $\gamma_W = P_M g_E/\sigma^2$, $\bar{\gamma}_W = P_M/(\sigma^2 \lambda_3)$ and $L_W = L_M = 1$ into Eq. (6) in [18], we can calculate $SOP_2(C_{th})$ as

$$SOP_2(C_{th}) = 1 - \frac{\bar{\gamma}_M}{(\bar{\gamma}_M + \alpha \bar{\gamma}_W)} \cdot \exp\left(-\frac{\alpha - 1}{\bar{\gamma}_M}\right). \quad (18)$$

As $g_P = |h_1|^2 \sim \exp(\lambda_P)$, the items $\Pr\{g_P \geq I_P/P_M\}$ and $\Pr\{g_P \leq I_P/P_M\}$ in (6) can be easily obtained as follows

$$\Pr\{g_P \geq I_P/P_M\} = \exp\left(-\frac{\lambda_P I_P}{P_M}\right), \quad (19)$$

$$\Pr\{g_P \leq I_P/P_M\} = 1 - \exp\left(-\frac{\lambda_P I_P}{P_M}\right), \quad (20)$$

respectively.

Finally, SOP can be obtained by substituting (19), (20), (17) and (18) into (6).

3.2 Log-normal fading channels

In this part, we assume that all links experience i.i.d. log-normal fading, $h_i \sim \log -N(\mu_i, \sigma_i^2)$ ($i \in \{1, 2, 3\}$), where μ_i and σ_i are the mean and variance for h_i 's natural logarithm, respectively.

Utilizing the properties of log-normal distribution (Property 1 in 22.10 of [19]), we have

$$|h_i|^2 \sim \log -N(2\mu_i, 4\sigma_i^2). \quad (21)$$

As suggested by (7), SOP can be given as

$$\Pr\{C_S \leq C_{th}\} = \Pr\left\{\frac{(\alpha - 1)g_P + \alpha \rho g_E}{\rho g_D} \geq 1\right\}. \quad (22)$$

3.2.1 The derivation of SOP_1

Let $Z_1 = (\alpha - 1)g_P$, $Z_2 = \alpha \rho g_E$, $Z_3 = \rho g_D$. The probability density function (PDF) of Z_1 , Z_2 and Z_3 can be given by

$$f_{Z_1}(z_1 | g_P \geq I_P/P_M) = \frac{f_{Z_1}(z_1)}{1 - F_{Z_1}((\alpha - 1)I_P/P_M)} = A f_{Z_1}(z_1), \quad (23)$$

$$Z_2 \sim \log -N(\mu_{Z_2}, \sigma_{Z_2}^2), \quad (24)$$

$$Z_3 \sim \log -N(\mu_{Z_3}, \sigma_{Z_3}^2), \quad (25)$$

where $f_{Z_1}(z_1) = \frac{1}{z_1 \sigma_{Z_1} \sqrt{2\pi}} \exp(-\frac{(\ln z_1 - \mu_{Z_1})^2}{2\sigma_{Z_1}^2})$ ($\mu_{Z_1} = 2\mu_1 + \ln(\alpha - 1)$, $\sigma_{Z_1}^2 = 4\sigma_1^2$), $F_{Z_1}(z_1) = \Phi(\frac{\ln z_1 - \mu_{Z_1}}{\sigma_{Z_1}})$ (Φ is the standard normal cumulative distribution function (CDF)) are the PDF and CDF of Z_1 , respectively, and $A = \frac{1}{1 - F_{Z_1}((\alpha - 1)I_P/P_M)}$, $\mu_{Z_2} = 2\mu_2 + \ln(\alpha \rho)$, $\sigma_{Z_2}^2 = 4\sigma_2^2$, $\mu_{Z_3} = 2\mu_3 + \ln \rho$, $\sigma_{Z_3}^2 = 4\sigma_3^2$.

Let $Y = Z_1 + Z_2$, then, the PDF of Y can be written as

$$f_Y(y) = A \int_0^\infty f_{Z_1}(x) f_{Z_2}(y - x) dx, \quad (26)$$

where $f_{Z_2}(z_2) = \frac{1}{z_2 \sigma_{Z_2} \sqrt{2\pi}} \exp(-\frac{(\ln z_2 - \mu_{Z_2})^2}{2\sigma_{Z_2}^2})$ is the PDF of Z_2 .

According to Fenton Wilkinson approximation [20], we can obtain that the distribution of the sum of two independently log-normal distributed variables can be approximated as a log-normal distribution. Thus, we have

$$\int_0^\infty f_{z_1}(x) f_{z_2}(y-x) dx \approx \frac{1}{y\sigma_Y\sqrt{2\pi}} \exp\left(-\frac{(\ln y - \mu_Y)^2}{2\sigma_Y^2}\right), \quad (27)$$

where

$$\sigma_Y^2 = \log \left[\frac{\sum_{i \in \{Z_1, Z_2\}} \exp(2\mu_i + \sigma_i^2) \exp(\sigma_i^2 - 1)}{\left[\sum_{i \in \{Z_1, Z_2\}} \exp\left(\mu_i + \frac{\sigma_i^2}{2}\right)\right]^2} + 1 \right]$$

and

$$\mu_Y = \log \left[\sum_{i \in \{Z_1, Z_2\}} \exp\left(\mu_i + \frac{\sigma_i^2}{2}\right) \right] - \frac{\sigma_Y^2}{2}.$$

Then, using (27) in (26), we have

$$f_Y(y) \approx \frac{A}{y\sigma_Y\sqrt{2\pi}} \exp\left(-\frac{(\ln y - \mu_Y)^2}{2\sigma_Y^2}\right). \quad (28)$$

Further, utilizing the properties of log-normal distribution (Property 1 in 22.10 of [19]), the PDF of $X = \frac{Y}{Z_3}$ can be given as

$$f_X(x) \approx A \int_0^\infty \frac{1}{y\sigma_Y\sqrt{2\pi}} \exp\left(-\frac{(\ln y - \mu_Y)^2}{2\sigma_Y^2}\right) f_{z_3}\left(\frac{y}{x}\right) dx = A \frac{1}{x\sigma_X\sqrt{2\pi}} \exp\left(-\frac{(\ln x - \mu_X)^2}{2\sigma_X^2}\right), \quad (29)$$

where $\mu_X = \mu_Y - \mu_{Z_3}$ and $\sigma_X^2 = \sigma_Y^2 + \sigma_{Z_3}^2$.

Therefore, $SOP_1(C_{th})$ can be expressed as

$$SOP_1(C_{th}) = \Pr \left\{ X = \frac{Z_1 + Z_2}{Z_3} \leq 1 \right\} \approx \int_0^1 A \frac{1}{x\sigma_X\sqrt{2\pi}} \exp\left(-\frac{(\ln x - \mu_X)^2}{2\sigma_X^2}\right) dx = A\Phi\left(-\frac{\mu_X}{\sigma_X}\right). \quad (30)$$

3.2.2 The derivation of $SOP_2(C_{th})$

When $g_P < I_P/P_M$ and $P_t = P_M$, it means that SU-TX only adopts its maximal transmitting power to deliver information to SU-RX. Obviously, the target system model falls into non-CR model in this case.

Utilizing the properties of log-normal distribution (Property 3 in 22.10 of [19]), we can obtain

$$\gamma_{S,i} = P_M |h_{S,i}|^2 / \sigma^2 \sim \log -N(\mu_{S,i}, \sigma_{S,i}^2), \quad i \in \{D, E\}, \quad (31)$$

where $\mu_{S,D} = 2\mu_2 + \ln(P_M/\sigma^2)$, $\sigma_{S,D}^2 = 4\sigma_2^2$, $\mu_{S,E} = 2\mu_3 + \ln(P_M/\sigma^2)$ and $\sigma_{S,E}^2 = 4\sigma_3^2$.

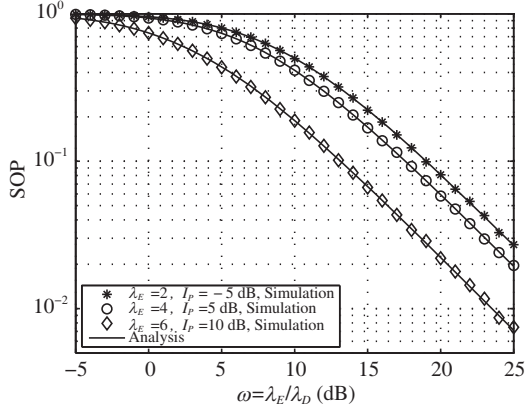
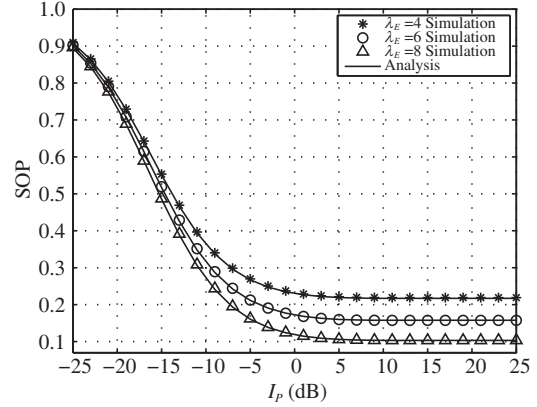
Then, making use of Eq. (26) in [21], $SOP_2(C_{th})$ can be obtained as

$$SOP_2(C_{th}) \approx 1 - \frac{2}{3}Q\left(\frac{\varphi(\mu_{\gamma_{S,E}}) - \mu_{\gamma_{S,D}}}{\sigma_{\gamma_{S,D}}}\right) - \frac{1}{6}Q\left(\frac{\varphi(\mu_{\gamma_{S,E}} + \sqrt{3}\sigma_{\gamma_{S,E}}) - \mu_{\gamma_{S,D}}}{\sigma_{\gamma_{S,D}}}\right) - \frac{1}{6}Q\left(\frac{\varphi(\mu_{\gamma_{S,E}} - \sqrt{3}\sigma_{\gamma_{S,E}}) - \mu_{\gamma_{S,D}}}{\sigma_{\gamma_{S,D}}}\right), \quad (32)$$

where $Q(x) = 1/\sqrt{2\pi} \int_x^\infty \exp(-t^2/2) dt$ and $\varphi(x) = \ln(\alpha \exp(x) + \alpha - 1)$.

As $g_P = |h_1|^2$ and using (21), the items $\Pr\{g_P < I_P/P_M\}$ and $\Pr\{g_P \geq I_P/P_M\}$ in (6) can be calculated as

$$\Pr\{g_P < I_P/P_M\} = \Phi\left(\frac{\ln(I_P/P_M) - 2\mu_1}{\sigma_1}\right), \quad (33)$$


Figure 2 SOP versus ω over Rayleigh fading channels.

Figure 3 SOP versus I_P over Rayleigh fading channels.

$$\Pr \{g_P \geq I_P/P_M\} = 1 - \Phi \left(\frac{\ln(I_P/P_M) - 2\mu_1}{\sigma_1} \right), \quad (34)$$

respectively.

Finally, the approximated expression of SOP over log-normal fading channels can be obtained by substituting (30), (32)–(34) into (6).

4 Numerical and simulation results

In this section, we present Monte Carlo simulation and analytical results corresponding to the secrecy outage over independent Rayleigh and log-normal fading channels. Unless otherwise explicitly specified, the parameters are set as $P_M = 1$ dB, $\sigma^2 = 1$, $I_P = 1$ dB, $\lambda_i = 1$ ($i \in \{P, D, E\}$), $\mu_i = 1$ ($i \in \{1, 2, 3\}$), $\sigma_i^2 = 1$ ($i \in \{1, 2, 3\}$) and $C_{th} = 0$ dB. During each simulation, S sends 4×10^6 bits to D .

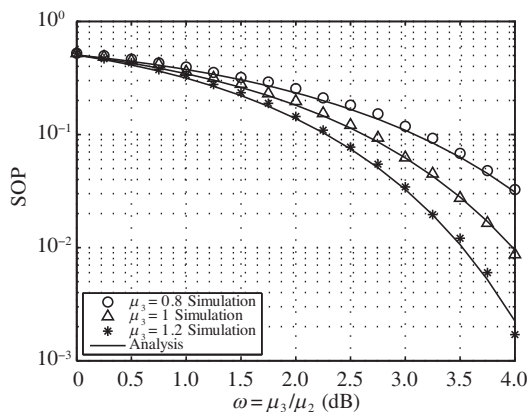
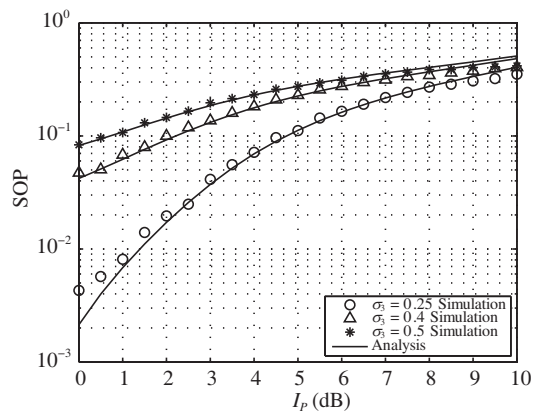
Figures 2 and 3 present the results for Rayleigh fading scenarios. It is seen that SOP has been improved while ω increases because a larger ω means a better $S - D$ link. Further, it can also be seen that the simulation results match very well with analytical results.

In Figure 2, we compare simulation and analytical results of SOP while $(\lambda_E, I_P) = (2, -5$ dB), $(4, 5$ dB) and $(6, 10$ dB). It could be observed that the SOP for a higher λ_E outperforms that of a higher λ_E as a higher λ_E represents a worse $S - E$ link.

Figure 3 describes the SOP versus I_P while $\lambda_E = 4, 6, 8$. We find that the SOP for a higher λ_E outperforms the one for a lower Γ . Similar reason with Figure 2 can be used to explain it. We can also find that SOP can be improved with the increasing of I_P . Because, when $P_M > I_P/g_P$, the transmitting power at S will increase as I_P increases, as suggested by Eq. (3). However, there is a floor in high I_P region. It is because the transmitting power at S cannot increase any more when $P_M < I_P/g_P$. Figures 4 and 5 present the results for log-normal fading scenarios. It is seen that the simulation results match very well with analytical results in most cases. We also can find that there is a mismatch between simulation and analytical results because of the adopted Fenton Wilkinson approximation [20] and the approximated result of the SOP in non-CR scenarios as suggested by Eq. (26) in [21].

In Figure 4, we compare simulation and analytical results of SOP versus ω (versus $\omega = \mu_3/\mu_2$) while $\mu_3 = 0.8, 1, 1.2$. SOP can be improved while ω is increasing, which means $S - D$ link gets better than $S - E$ link. Further, we can see that SOP for a higher μ_3 outperforms that of a lower μ_3 .

In Figure 5, SOP versus I_P is described while $\omega = \mu_3/\mu_2$ is with the same value of I_P . It is clear that the SOP with a lower γ_3 outperforms the one with a higher γ_3 , as a higher γ_3 represents a worse $S - E$ link condition, which results in a lower SOP. Moreover, we can also observe that SOP gets worse while I_P and ω are increasing. Because $S - D$ link gets worse compared to $S - E$ link when ω increases.

Figure 4 SOP versus ω over log-normal fading channels.Figure 5 SOP versus I_P over log-normal fading channels.

5 Conclusion

In this paper, we have investigated the secrecy outage performance for the spectrum sharing system over independent Rayleigh and log-normal fading channels. The closed-form and approximated expressions for secrecy outage probability over Rayleigh and log-normal fading channels have been respectively derived. The simulation results show good agreement with analytical results obtained in this work.

Acknowledgements This research was supported in part by National Natural Science Foundation of China (Grant Nos. 61401372, 61531016), Research Fund for the Doctoral Program of Higher Education of China (Grant No. 20130182120017), Natural Science Foundation Project of CQ CSTC (Grant No. cstc2013jcyjA40040), Fundamental Research Funds for the Central Universities (Grant No. XDJK2015B023), and National Undergraduate Training Programs for Innovation and Entrepreneurship (Grant No. 201410635005).

Conflict of interest The authors declare that they have no conflict of interest.

References

- Wyner D. The wire-tap channel. *Bell Syst Tech J*, 1975, 54: 1355–1367
- Bloch M, Barros J, Rodrigues M R D, et al. Wireless information theoretic security. *IEEE Trans Inf Theory*, 2008, 54: 2515–2534
- Liu T, Shamai S. A note on the secrecy capacity of the multiple-antenna wiretap channel. *IEEE Trans Inf Theory*, 2009, 55: 2547–2553
- Li Q, Song H, Huang K. Achieving secure transmission with equivalent multiplicative noise in MISO wiretap channels. *IEEE Commu Lett*, 2013, 17: 892–895
- Li Q, Ma W-K, Man-Cho So A. A safe approximation approach to secrecy outage design for MIMO wiretap channels. *IEEE Sig Process Lett*, 2014, 21: 118–121
- Sun X, Wang J, Xu W, et al. Performance of secure communications over correlated fading channels. *IEEE Sig Process Lett*, 2012, 19: 479–482
- Liu X. Secrecy capacity of wireless links subject to log-normal fading. In: *Proceedings of 7th International Conference on Communications and Networking in China*, Kunming, 2012. 167–172
- Zhang X, Pan G, Tang C, et al. Performance analysis of physical layer security over independent/correlated log-normal fading channels. In: *Proceedings of Australasian Telecommunication Networks and Applications Conference*, Melbourne, 2014. 23–27
- Zahurul M, Sarkar I, Ratnarajah T. Secrecy capacity over correlated log-normal fading channel. In: *Proceedings of IEEE International Conference on Communications*, Ottawa, 2012. 883–887
- Mitola J. Cognitive radio: an integrated agent architecture for software defined radio. Dissertation for Ph.D. Degree. Stockholm: KTH, 2000
- Shu Z, Qian Y, Ci S. On physical layer security for cognitive radio networks. *IEEE Netw*, 2013, 27: 28–33
- Zou Y, Wang X, Shen W. Physical-layer security with multiuser scheduling in cognitive radio networks. *IEEE Trans Commu*, 2013, 61: 5103–5113
- Sakran H, Shokair M, Nasr O, et al. Proposed relay selection scheme for physical layer security in cognitive radio networks. *IET Commun*, 2012, 6: 2676–2687

- 14 Wen H, Li S, Zhu X, et al. A framework of the PHY-layer approach to defense against security threats in cognitive radio networks. *IEEE Netw*, 2013, 27: 34–39
- 15 Tang C, Pan G, Li T. Secrecy outage analysis of underlay cognitive radio unit over Nakagami- m fading channels. *IEEE Wirel Commun Lett*, 2014, 3: 609–612
- 16 Elkashlan M, Wang L, Duong T Q, et al. On the security of cognitive radio networks. *IEEE Trans Veh Technol*, 2015, 64: 3790–3795
- 17 Papoulis A. *Probability, Random Variables and Stochastic Processes*. 4th ed. New York: McGraw Hill, 2001
- 18 He F, Man H, Wang W. Maximal ratio diversity combining enhanced security. *IEEE Commun Lett*, 2011, 15: 509–511
- 19 Krishnamoorthy K. *Handbook of Statistical Distributions with Applications*. New York: Chapman & Hall, 2006
- 20 Fenton L. The sum of log-normal probability distributions in scatter transmission systems. *IRE Trans Commun Syst*, 1960, 8: 57–67
- 21 Pan G, Tang C, Zhang X, et al. Physical layer security over non-small scale fading channels. *IEEE Trans Veh Tech*, 2016, 65: 1326–1339